The Generation and *In situ* Electrochemical Detection of Transient Nanobubbles

Peter R. Birkin[†*], Steven Linfield[†], Jack J. Youngs[†] and Guy Denuault[†]

†Department of Chemistry, University of Southampton, Southampton, United Kingdom, SO17 1BJ

Supporting Information Placeholder

ABSTRACT: Nanobubbles are fascinating but controversial objects. Although there is strong evidence for the existence of surface bound nanobubbles, the possibility of stable nanobubbles in the bulk remains in question. In this work, we show how ultrasonication of electrolytes can create transient bulk nanobubbles. To do this, glass nanopores are used as Coulter counters in order to detect nanobubbles. During ultrasonication, these transient bulk nanobubbles are shown to exist in relatively high concentrations while bubble activity on the surface of a solid media close to the pore is driven by ultrasound. However, the transient nature of these bubbles is evident upon termination of the ultrasonic source. High-speed imaging suggests that these transient nanobubbles originate from the fragmentation of larger bubbles, which skate over the surface of the structure in the acoustic field present. Transient nanobubbles as small as ~100 nm diameter are detected. In contrast to previous work with microbubbles, no evidence for the oscillation of these nanobubbles during translocation was found. The novel experimental approach presented here provides strong evidence for the existence of transient nanobubbles in bulk solution.

Keywords: transient bulk nanobubbles; bubble fragmentation; acoustic cavitation; nanopore detection

Nanobubbles have a long history and were first described as nuclei in bulk solution[1] in 1962 and on surfaces[2] in 1994. While many potential applications of nanobubbles have been proposed (e.g. membrane cleaning[3], drug delivery[4], and froth flotation[5]), their existence and apparent long stability have attracted considerable interest[6]. However, before these benefits can be fully exploited, the debate as to whether these nanobubbles actually exist has to be fully addressed. Key to this debate are the well-known properties of bubbles within liquids. For example, bubbles are inherently unstable and, will ultimately be removed from the liquid through either dissolution, coalescence or conventional buoyancy under the influence of gravity. The latter mechanism is particularly rapid as bubbles become larger. For smaller bubbles, dissolution is thought to be rapid. The lifetime of a bubble has been predicted by Epstein and Plesset[7]. Here under typical conditions, a 1 μm diameter bubbles would be expected to dissolve in ~9.5 ms in air saturated media. Ultimately, the driving force for this apparent instability is the Laplace pressure, which increases as the bubble size decreases. This effect has been termed the Laplace catastrophe[8]. These observations suggest that nanobubbles should be extremely susceptible to dissolution, but published experimental data suggest that they are stable enough to be observed experimentally[9]. It is important to note that there are clear distinctions between bubbles at the solid/liquid interface and those in the bulk solution. Evidence for the existence of multiple surface bound nanobubbles which have been shown to be gas filled[10], and single nanobubbles on nanoelectrodes has been reported (e.g. with atomic force[11] and optical microscopy[12]). The reasons for the stability and the effects of solution parameters (e.g. salt concentrations and the deliberate addition of surfactant materials have been reported (see ref[8] for a good review of the available literature). While the number of studies and the proposed mechanisms of stability are well developed for surface bound bubbles (some created electrochemically[13,14]), the evidence for and the stability mechanisms are not accepted for nanobubbles in the bulk. Bulk nanobubbles have been examined with dynamic light scattering[3] and displacement instruments. Changes in the overall size as a function of time (through growth and dissolution mechanisms) have been proposed[15]. Nuclear magnetic resonance has even been used to study the effect of nanobubbles on the spin relaxation time[16]. In addition, scanning electron microscopy has been employed to study frozen solution containing bubbles[9,17]. These reports suggest that the evidence is mounting for the existence of bulk nanobubbles; however, questions remain as to their ultimate stability. In order to answer some of these questions experimental observations, which detect, identify, size and track sub-micrometer bubbles are important. It would also be advantageous to control the generation of nanobubbles in order to probe their stability and lifetime. Correlating the measured signals with their generation would also help discriminate against contaminating particles. Hence, a combination of detection and generation techniques would be extremely powerful. Here we use *in situ* Coulter counting in combination with bubble generation through the application of power ultrasound[18].

Coulter counting[19] is an analytical electrochemical technique that allows for the detection of particles, microbes, polymers, and bubbles. This technique works by applying a voltage between two electrodes on either side of a suitable pore. The resulting ionic current flows through the pore but is limited by the pore resistance. As a particle enters the pore, it displaces the electrolyte and therefore increases the resistance of the pore momentarily[20]. This can be witnessed by recording the current passing through the pore. It is possible to derive information from the change in current signal, the duration and shape of the signal, and the frequency of the events[21]. Considering the dimensions of nanobubbles, it is advantageous to use pores of similar dimensions. Hence, we have developed a set of nanopores, based on a modified literature fabrication technique, to produce glass nanopores[22–24] (GNP).

In this work, we report the use of Coulter counting with nanopores as a new method to detect and characterize bulk nanobub-

bles. We use ultrasonication to control the generation of the nanobubbles and show that they can be sized from the magnitude of the translocation signal, that they appear not to oscillate and that they disappear on termination of the driving generation mechanism.

EXPERIMENTAL DETAILS

Chemicals and Materials: Potassium chloride (99.5%) and sodium hydroxide (97%) were purchased from Fischer Scientific, $[Ru(NH_3)_6]Cl_3$ (99%) from Strem and potassium persulfate (98%) from Lancaster Synthesis. All chemicals were used as received and all solutions were made with 18.2 MΩ cm purified water from a Suez Select Fusion water system. Tungsten microwire (diameter 25 µm, 99.5%) was purchased from Advent Research Materials. Emery paper (P600 and P1200) and lapping films (5, 1, and 0.3 µm) were purchased from 3M. 22% PbO glass capillaries (PG10165-4, OD 1.65 mm, ID 1.1 mm) were purchased from World Precision Instruments.

Conical nanopores[25] were prepared by electrochemically etching tungsten 25 µm diameter microwires in 2 M NaOH before sealing them in 22% PbO glass capillaries. The electrochemical etching process was controlled by a specialized circuit designed to terminate the electrochemical current if it fell below ~0.3 mA. This ensured that the tip remained relatively sharp with a tip radius ~10 nm and a cone angle of ~ 3-5° (determined by FEGSEM). This tip was then embedded in a PbO glass capillary in a flame. The tip of the wire was exposed by polishing using a custom made continuity tester (see ref[24] for further details). Sizing of the resultant nanoelectrodes was performed using voltammetry of $Ru(NH_3)_6^{3+}$. The W template was then removed by chemical etching in a solution containing 250 mM $K_2S_2O_8$ and 2 M NaOH. The fully developed nanopore was then characterized by investigating the i-V curve in a solution of 1 M KCl. Note that in order to increase the certainty of the size of the nanopore, the voltammetry of the nanoelectrodes (prior to chemical etching to produce the pore) was combined with the i-V characteristics in electrolytes. This enabled an estimation of the cone angle and pore mouth of each nanopore without reliance on microscopy. Further details on the errors associated with this process can be found in the SI (see Figure S4).

Electrochemical measurements were performed with a custom-made two-electrode potentiostat, capable of recording current ranges as low as 1 pA. Ion current results were recorded using a custom-made current follower with a gain of up to 10^9 V/A. This system was constructed following a similar protocol to that reported by Sigworth[26]. Further details of the approach adopted and the performance of the device is included in the SI data (see Figure S5).

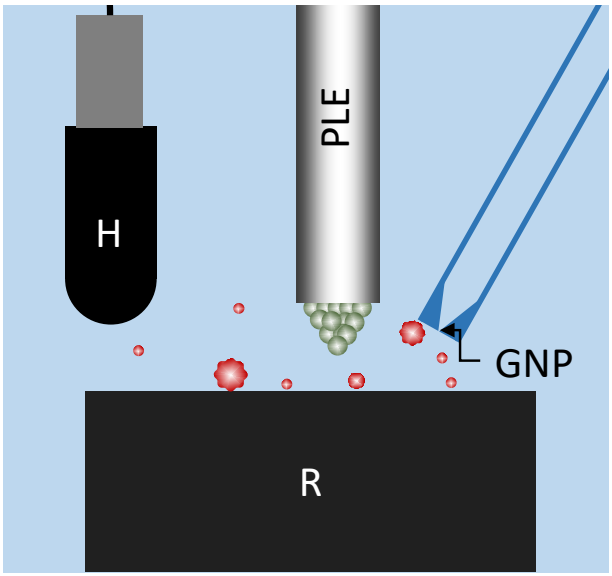

Figure 1. Schematic representation of the generation and detection of nanobubbles. Here the sound source (a piston like emitter, PLE) was positioned over a glass reflector (R). The GNP, shown on the right of the image, and the hydrophone (H) were held in position by appropriate mechanical stands. Note, this is not to scale. Different bubble activity is also highlighted including the cluster[27,28] (●) at the end of the PLE and bubbles in the bulk or on the surfaces (●). Note the jagged edges on some bubbles are a pictorial representation of those bubbles, which exhibit surface wave oscillation. See SI figure S1.

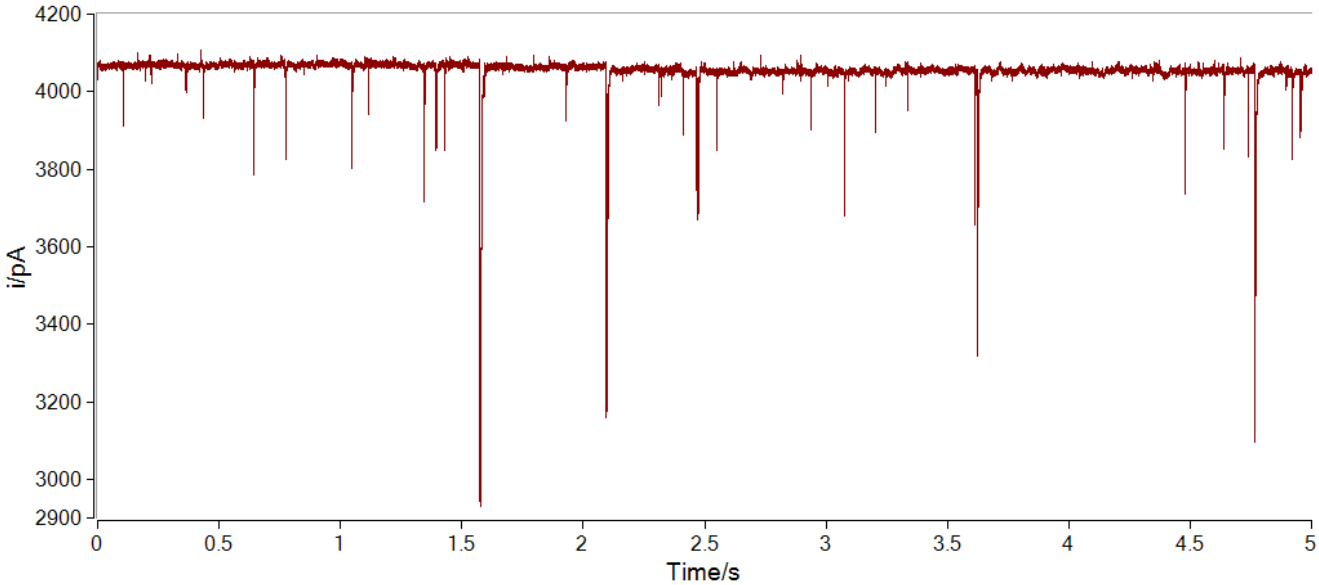

Figure 2. Plot showing the ion current (i, —) as a function of time for a 440 nm diameter pore. The GNP was positioned ~1 mm laterally and level with the PLE (2 W_{rms}). The aerobic solution contained 10 mM KCl. A potential of 280 mV was applied across the pore. A pressure difference of 77 mBar was applied to draw liquid into the GNP. The solution temperature was ~28 °C.

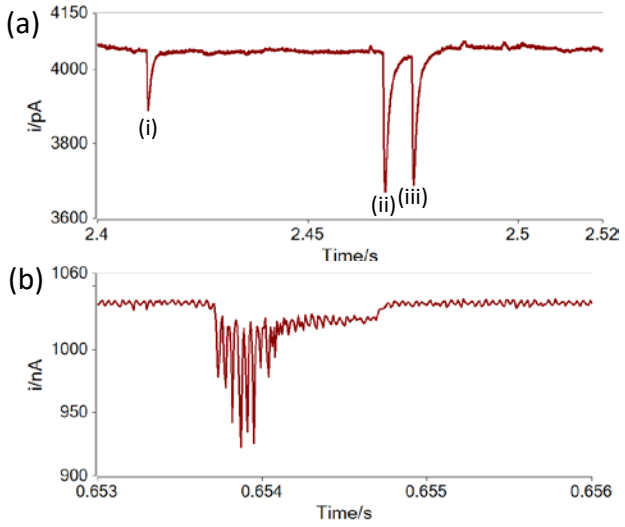

Figure 3. Plots showing the ion current (i, —) as a function of time for (a) a 440 nm diameter GNP and (b) a 40 µm GMC. The pores were positioned ~1 mm laterally and level with the PLE (2 W_{rms}). The aerobic solution contained 10 mM KCl. A potential of 280 mV and 5 V was applied across the GNP and a glass microchannel respectively. A pressure difference of 75-77 mBar was applied to draw liquid into the pores. The solution temperature was ~28 °C.

High-speed camera videos were recorded using a Fastcam-APX RS from Photron. A 12X Navitar lens with a variable 0.58X-7X zoom and a .67X adaptor tube was fitted onto the camera unit. The videos were analysed using Photron Fastcam Viewer ver. 3391 software.

Ultrasonication of potassium chloride solutions was achieved using a titanium piston like emitter (PLE) fitted with an insulating ABS thread. The PLE was powered by a Microson XL2007 ultrasonic cell disruptor from Misonix Inc. The PLE frequency was ~22-23 kHz and, unless specified, the PLE was driven at an output power (reported by the instrumentation) included in the appropriate figure legend. The potassium chloride solutions were held in a custom cell fitted with an optical glass window for the high-speed camera to observe the bubbles. An SQ16 joint at the bottom of the cell allowed a 1 cm diameter glass cylinder to be inserted at variable height. The tip of the PLE (Ti, 3.2 mm diameter) was held 2.5 mm above the glass cylinder and 5 mm below the meniscus of the solution.

Figure 1 shows the experimental setup used in this study. Here the PLE was used to create a large bubble population within the fluid. It was found to be advantageous to use the glass cylinder as a reflector (R) as this improved the frequency of bubble detection. The hydrophone (H) was used to monitor the acoustic conditions within the cell.

RESULTS AND DISCUSSION

Figure 2 shows the current time history of a 440 nm diameter GNP in the presence of ultrasound. Here, the GNP was positioned so that it was ~ 2 mm horizontally from the operating PLE. Figure 2 shows many transient drops in the current passed through the nanopore. These are attributed to the passage of insulating material through the GNP and are assigned to the translocation of nanobubbles produced by the sound source outside the GNP. This is supported by consideration of the dimensions of the nanopore (estimated to be 440 nm in diameter from the electrochemical characterization, see SI for discussion) and the magnitude of the current change detected (Δi up to ~1100 pA). The range of current transients detected suggests that there is a broad distribution of bubble sizes transferring through the GNP. Figure 3 (a) shows the current time history for three specific translocations. In each case, the current transient is characterized by a rapid decrease in the current followed by a slower relaxation of the current back to the baseline (here ~4070 pA). Assuming that the pore dimensions were accurate (note the cone angle for these structures was estimated by looking at the voltammetry of the W nanoelectrodes prior to etching and then comparing to the ion current, see SI for further details), it is possible to size these events. For example, events (i), (ii) and (iii) correspond to bubbles (by appropriate comparison to simulation of the system, see SI, Figure S6) with a diameter of 256 nm, 326 nm and 324 nm respectively. For comparison, Figure 3(b) shows how the ionic current changes when a microbubble translocates through a glass microchannel (GMC). Some clear differences should be noted from this data.

Figure 3 (a) shows that the shape of the translocation event is significantly different with the nanobubbles translocation exhibiting an asymmetric fall and rise in current compared to the microbubble case. These nanobubble translocation transients are similar to those obtained when polystyrene nanospheres translocate through nanopores (see SI data, Figure S8). However, the Coulter counter current for microbubble translocations is significantly different. Figure 3 (b) shows that microbubble translocation is accompanied with current oscillations which have been shown to be linked to the local acoustic environment[29]. In essence, the microbubbles oscillate in the sound field present as they translocate. This dynamic size change can be detected by measurement of the ion current through the micropore. However, no such oscillation can be seen in the GNP case. This suggest that these nanobubbles do not oscillate significantly, as they pass through the GNP. However, some caution must be noted here, as the instrumentational limitations of the system need to be considered. In the case of the GNP system, a current follower with a gain of 10^9 V A^{-1} was employed. This could be limiting as the transients are of ms duration. However, analysis of the performance of this system (see SI data, Figure S4 and discussion) suggests that this device was not significantly altering the shape of the current time transients recorded. If this is the case, the absence of nanobubbles oscillation is intriguing.

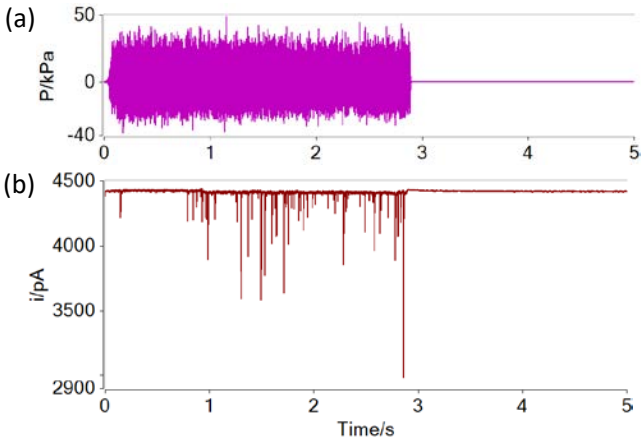

Figure 4. Plots showing the ion current (i, —) for a 440 nm diameter pore and the acoustic pressure (P, —) as a function of time. The GNP was positioned ~1 mm laterally and level with the PLE (6 W_{rms}). The aerobic solution contained 10 mM KCl. A potential of +350 mV was applied across the pore. A pressure difference of 76 mBar was applied to draw liquid into the GNP. The solution temperature was ~23.5 °C.

First, one possibility is that these bubbles are far from resonance at 23 kHz (a 100 nm radius bubble would be expected[30] to have a

resonance frequency of the order of 85 MHz). Hence, the degree of oscillation expected would be much smaller than that expected for the microbubble case (see calculations in SI, Figure S7, which supports this conclusion). Second, the forces, damping and structure of the bubble wall (which are a matter of interest), may restrict the motion of these structures. Further work is needed to determine the dynamics of these bubbles, but this will require a more refined experimental approach.

While the evidence suggests the presence of nanobubbles within this system, a measure of their stability would be useful. Figure 4 shows the ion current and acoustic pressure within the cell as nanobubbles where generated (through the action of ultrasound) during and after the termination of the ultrasonic field. Figure 4 (a) shows that the acoustic field was initiated at 0 s and active to ~3 s in this experiment. While the sound field is active (At time < ~3 s), figure 4 (b) shows the characteristic signature of nanobubbles translocating through the GNP. However, on termination of the sound source, detection of the translocation events also stopped. This suggests that while the sound source was active, nanobubbles were present and produced by mechanisms present in this environment, including presumably fragmentation effects[31]. However, as soon as the source was terminated, these bubbles were no longer detected. Figure 4, which was found to be reproducible over multiple runs and experiments, provides strong evidence that the translocation events are related to transient nanobubbles and not to nanoparticles present in the electrolyte. Several possibilities exist as to the cause of this phenomenon. First, the actual bulk concentration of nanobubbles in the media is extremely low and events are rare in the absence of the generating mechanism (here the ultrasonic source and the associated bubbled activity). Second, the nanobubbles that were produced shrink rapidly to a size, which is no longer detectable in the GNP (note, entities with a radius smaller than ~80 nm would not be detected when translocating through a 440 nm pore under the conditions employed, see SI, Figure S6). Third, the transient nanobubbles are ephemeral in nature and disappear through standard dissolution processes[7] driven by the physical forces present. Nevertheless, the data suggests that an intermediary nanobubble stage is detectable and, considering that a nanobubble generation mechanism is likely to produce such entities regardless of their ultimate fate, these observations provide key evidence for the production of bulk transient nanobubbles even if this cannot prove their final existence.

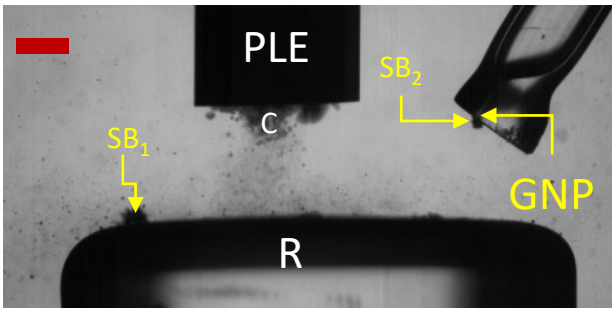

Figure 5. Image showing the experimental system while bubble activity is driven by the PLE. A cluster (C) is seen at the PLE tip; bubble activity in the liquid, on the surface of the reflector (R) and GNP support is apparent. Two surface confined bubbles ($SB_{1,2}$) are highlighted, with SB_2 close to the GNP mouth. The scale bar represents 1 mm. In this case, the edge of the GNP was ~ 1.8 mm from the edge of the PLE.

In order to understand the generation mechanisms present, high-speed imaging of the GNP and the local environment was undertaken. Clearly, imaging the bubbles (of the order of 100 nm in diameter) is challenging. However, the local conditions (in terms of microbubbles etc.) are possible to image. Figure 5 shows an image of the bubble activity generated under the conditions we employed. It was observed (see SI data, Movie S1 for high-speed imaging data) that nanobubbles translocation through the GNP was accompanied by the presence of dynamic surface confined microbubbles which skated over the GNP structure. This suggests that fragmentation of these larger gas bubbles is the origin of these transient nanobubbles. In contrast to work on microbubbles[29], the GNP is unable to draw these surface bubbles through the pore opening (under the conditions employed). Hence, the surface confined bubbles were observed to continuously skate over the structure producing the nanobubbles signature. Termination of the sound source resulted in loss of activity of these bubbles and a concomitant loss in transient nanobubbles detection (see figure 4). In some cases, a permanent (on the time scale of the imaging) bubble (diameter ~ 150 µm) was left on the surface of the GNP structure (see SI data, Figure S1). In the experimental investigation, a pressure difference (of the order of 80 mbar) was applied across the pore. However, other factors, such as electroosmosis and electrophoresis, could be a contributory effect when considering the translocation of particles or indeed nanobubbles through these structures. These effects, for particles, have been discussed in several careful and elegant investigations of nanoparticles translocation through asymmetric channels[23,32,33] (see ref[23] for an excellent review of the topic). In the current study, we observed similar translocation events for both positive and negative polarities across the nanopores used (see SI data, Figure S9). However, accessing force balance effects and associated velocities remain an intriguing question in relation to the bubble size, inherent charge, the pore wall, the nanopores size, the solution conditions, the magnitude of the potential applied across the nanopore and the possible transient nature of the population of bubbles produced under the conditions employed in this investigation. Lastly, under the conditions employed (e.g. the pressure differential and the exposure to the ultrasonic field etc.) the nanopore remained clear of obstructions.

CONCLUSIONS

Transient nanobubbles can be sensed within an electrolyte exposed to ultrasound. These are detected as changes in the ion current passing through a GNP. These nanobubbles appear to originate from the fragmentation of a microbubble skating over the surface of the glass support of the GNP. In contrast to microbubbles, which are driven to oscillate during translocation by the local acoustic field, no oscillation of the nanobubbles could be detected during translocation. Importantly, no translocation events could be detected in the absence of the generating conditions, thereby ruling out the involvement of bulk nanoparticles.

ASSOCIATED CONTENT

Supporting Information

A pdf file containing details of the experimental setup, FFT analysis of the current time data and estimation of errors associated with the GNP system is available in the SI. In addition, a set of high-speed imaging data (as an avi file, is available.) The Supporting Information is available free of charge on the ACS Publications website.

AUTHOR INFORMATION

Corresponding Author

Dr Peter Birkin, School of Chemistry, University of Southampton, Highfield, Southampton, SO171BJ, UK. prb2@soton.ac.uk.

Author Contributions

PRB conceived the nanopore system and ultrasonic generation protocol, GD advised on the project and SL & JY undertook the experimental study.

ACKNOWLEDGMENT

The authors are grateful to the University of Southampton for funding SL's PhD project and to the EPSRC for an equipment grant associated with the high-speed camera (EP/D05849X/1).

REFERENCES

(1) Sette, D.; Wanderlingh, F. Nucleation by Cosmic Rays in Ultrasonic Cavitation. *Phys. Rev.* **1962**, *125*, 409–417.

(2) Parker, J. L.; Claesson, P. M.; Attard, P. Bubbles, Cavities, and the Long-Ranged Attraction between Hydrophobic Surfaces. *J. Phys. Chem.* **1994**, *98*, 8468–8480.

(3) Zhu, J.; An, H.; Alheshibri, M.; Liu, L.; Terpstra, P. M. J.; Liu, G.; Craig, V. S. J. Cleaning with Bulk Nanobubbles. *Langmuir* **2016**, *32*, 11203–11211.

(4) Wang, Y.; Li, X.; Zhou, Y.; Huang, P.; Xu, Y. Preparation of Nanobubbles for Ultrasound Imaging and Intracelluar Drug Delivery. *Int. J. Pharm.* **2010**, *384*, 148–153.

(5) Calgaroto, S.; Wilberg, K. Q.; Rubio, J. On the Nanobubbles Interfacial Properties and Future Applications in Flotation. *Miner. Eng.* **2014**, *60*, 33–40.

(6) Ljunggren, S.; Eriksson, J. C. The Lifetime of a Colloid-Sized Gas Bubble in Water and the Cause of the Hydrophobic Attraction. *Colloids Surfaces A Physicochem. Eng. Asp.* **1997**, *129–130*, 151–155.

(7) Epstein, P. S.; Plesset, M. S. On the Stability of Gas Bubbles in Liquid-Gas Solutions. *J. Phys. Chem.* **1950**, *18*, 1505–1509.

(8) Alheshibri, M.; Qian, J.; Jehannin, M.; Craig, V. S. J. A History of Nanobubbles. *Langmuir* **2016**, *32*, 11086–11100.

(9) Uchida, T.; Liu, S.; Enari, M.; Oshita, S.; Yamazaki, K.; Gohara, K. Effect of NaCl on the Lifetime of Micro- and Nanobubbles. *Nanomaterials* **2016**, *6*, 1–10.

(10) Zhang, X. H.; Khan, A.; Ducker, W. A. A Nanoscale Gas State. *Phys. Rev. Lett.* **2007**, *98*, 1–4.

(11) Ishida, N.; Inoue, T.; Miyahara, M.; Higashitani, K. Nano Bubbles on a Hydrophobic Surface in Water Observed by Tapping-Mode Atomic Force Microscopy. *Langmuir* **2000**, *16*, 6377–6380.

(12) Xing, Z.; Wang, J.; Ke, H.; Zhao, B.; Yue, X.; Dai, Z.; Liu, J. The Fabrication of Novel Nanobubble Ultrasound Contrast Agent for Potential Tumor Imaging. *Nanotechnology* **2010**, *21*, 1–8.

(13) Luo, L.; White, H. S. Electrogeneration of Single Nanobubbles at Sub-50-Nm-Radius Platinum Nanodisk Electrodes. *Langmuir* **2013**, *29*, 11169–11175.

(14) Lemay, S. G. Noise as Data: Nucleation of Electrochemically Generated Nanobubbles. *ACS Nano* **2019**, *13*, 6141–6144.

(15) Kikuchi, K.; Ioka, A.; Oku, T.; Tanaka, Y.; Saihara, Y.; Ogumi, Z. Concentration Determination of Oxygen Nanobubbles in Electrolyzed Water. *J. Colloid Interface Sci.* **2009**, *329*, 306–309.

(16) Ushikubo, F. Y.; Furukawa, T.; Nakagawa, R.; Enari, M.; Makino, Y.; Kawagoe, Y.; Shiina, T.; Oshita, S. Evidence of the Existence and the Stability of Nano-Bubbles in Water. *Colloids Surfaces A Physicochem. Eng. Asp.* **2010**, *361*, 31–37.

(17) Wang, Q.; Zhao, H.; Qi, N.; Qin, Y.; Zhang, X.; Li, Y. Generation and Stability of Size-Adjustable Bulk Nanobubbles Based on Periodic Pressure Change. *Sci. Rep.* **2019**, *9*, 1–9.

(18) Kim, J. Y.; Song, M. G.; Kim, J. D. Zeta Potential of Nanobubbles Generated by Ultrasonication in Aqueous Alkyl Polyglycoside Solutions. *J. Colloid Interface Sci.* **2000**, *223*, 285–291.

(19) Coulter, W. H. Means for Counting Particles Suspended in a Fluid. *U.S. Pat.* **1953**, No. 2,656,508, 9.

(20) DeBlois, R. W.; Bean, C. P. Counting and Sizing of Submicron Particles by the Resistive Pulse Technique. *Rev. Sci. Instrum.* **1970**, *41*, 909–916.

(21) Lan, W.-J.; Holden, D. a.; Liu, J.; White, H. S. Pressure-Driven Nanoparticle Transport across Glass Membranes Containing a Conical-Shaped Nanopore. *J. Phys. Chem. C* **2011**, *115*, 18445–18452.

(22) Lan, W.-J.; Holden, D. A.; Liu, J.; White, H. S. Pressure-Driven Nanoparticle Transport across Glass Membranes Containing a Conical-Shaped Nanopore. *J. Phys. Chem. C* **2011**, *115*, 18445–18452.

(23) Luo, L.; German, S. R.; Lan, W.-J.; Holden, D. A.; Mega, T. L.; White, H. S. Resistive-Pulse Analysis of Nanoparticles. *Annu. Rev. Anal. Chem.* **2014**, *7*, 513–535.

(24) Zhang, B.; Galusha, J.; Shiozawa, P. G.; Wang, G.; Bergren, A. J.; Jones, R. M.; White, R. J.; Ervin, E. N.; Cauley, C. C.; White, H. S. Bench-Top Method for Fabricating Glass-Sealed Nanodisk Electrodes, Glass Nanopore Electrodes, and Glass Nanopore Membranes of Controlled Size. *Anal. Chem.* **2007**, *79*, 4778–4787.

(25) Wei, C.; Bard, A. J.; Feldberg, S. W. Current Rectification at Quartz Nanopipet Electrodes. *Anal. Chem.* **1997**, *69*, 4627–4633.

(26) Sigworth, F. J. Electronic Design of the Patch Clamp. In *Single Channel recording*; 1995; pp 95--127.

(27) Hansson, I.; Kedrinskii, V.; Morch, K. A. On the Dynamics of Cavity Clusters. *J. Appl. Phys. D Appl. Phys.* **1982**, *15*, 1725–1734.

(28) Hansson, I.; Morch, K. A. The Dynamics of Cavity Clusters in Ultrasonic (Vibratory) Cavitation Erosion. *J. Appl. Phys.* **1980**, *51*, 4651–4658.

(29) Birkin, P. R.; Linfield, S.; Denuault, G. The In Situ Electrochemical Detection of Microbubble Oscillations during Motion through a Channel. *PCCP* **2019**, *21*, 24802–24807.

(30) Walton, A. J.; Reynolds, G. T. Sonoluminescence. *Adv. Phys.* **1984**, *33*, 595.

(31) Watson, Y. E. Electrochemical Investigation of Bubble Wall Motion during Non-Inertial Cavitation. University of Southampton 2003.

(32) German, S. R.; Luo, L.; White, H. S.; Mega, T. L. Controlling Nanoparticle Dynamics in Conical Nanopores. *J. Phys. Chem. C* **2013**, *117*, 703–711.

(33) Arjmandi, N.; Van Roy, W.; Lagae, L.; Borghs, G. Measuring the Electric Charge and Zeta Potential of Nanometer-Sized Objects Using Pyramidal-Shaped Nanopores. *Anal. Chem.* **2012**, *84*, 8490–8496.

TOC graphic